J Nanostruct 15(4): 1535-1545, Autumn 2025

RESEARCH PAPER

Synthesis, Characterization and Study the Biological Activity for New Schiff Base Compound 2-(((1E,2E)-1,2-Diphenyl-2-((4-(E-1-(Thiazol-2-ylimino) Ethyl) Phenyl) Imino) Ethylidene) Amino) Phenol (DEAP)

Makarim A. Mahdi, Layth S. Jasim *, Hayder O. Jamel

Department of Chemistry, College of Education, University of Al-Qadisiyah, Iraq

ARTICLE INFO

Article History:
Received 18 June 2025
Accepted 04 August 2025
Published 01 October 2025

Keywords:
Biological Activity
Heterocyclic compound
Schiff base

ABSTRACT

The synthesis of the Schiff base compound (DEAP) 2-(((1E,2E)-1,2-diphenyl-2-((4-(E-1-(thiazol-2-ylimino) ethyl) phenyl)imino) ethylidene)amino)phenol ($C_{31}H_{24}N_4OS$) was successfully executed via a two-step condensation reaction. The preliminary step involved generating compound (A) (E)-4-(1-(thiazo-2-ylimino)ethyl)aniline, using 2-aminothiazol and 4-aminoacetophenone. The secondary step involved the synthesis of compound (DEAP) from compound (A), benzil, and 2-aminophenol. Various spectral techniques, such as Elemental analysis (C.H.N), ^{1}H,^{13}C-NMR, Mass spectrum, UV-Vis, FT-IR, XRD, and FE-SEM were employed for structural analysis of DEAP. Furthermore, the biological activities of the compound were scrutinized, with microbial susceptibility tests conducted on five isolates: Staphylococcus aureus, streptococcus mutans, pseudomonas aeruginosa, E. coli, and candida albicans, using the microtiter plate to determine the MIC. Anticancer potential of DEAP was investigated via cell cytotoxicity trials and in vitro antitumor screening against prostate cancer line PC3 and breast cancer (MCF-7) cell lines, utilizing the colorimetric (MTT) assay for evaluating cellular viability. The findings indicate selective cytotoxicity of DEAP, detrimental to cancerous cell lines while sparing normal cells, marking it as a prospective candidate for future cytotoxic therapies. Hence, further investigation into DEAP's potential as an anticancer drug is warranted.

How to cite this article
Mahdi M., Jasim L., Jamel H. Synthesis, Characterization and Study the Biological Activity for New Schiff Base Compound 2-(((1E,2E)-1,2-Diphenyl-2-((4-(E-1-(Thiazol-2-ylimino) Ethyl) Phenyl) Imino) Ethylidene) Amino) Phenol (DEAP). J Nanostruct, 2025; 15(4):1535-1545. DOI: 10.22052/JNS.2025.04.004

INTRODUCTION

Heterocyclic compounds, organic compounds with at least one carbon atom linked to a different atom (typically oxygen, nitrogen, or sulfur), have been extensively examined due to the abundance and variety of their natural or industrially synthesized derivatives [1, 2]. Among these, Schiff bases (or imines or azomethines), which are nitrogen analogs of aldehydes or ketones where the carbonyl group (CO) is substituted by an imine or azomethine group, exhibit various pharmacological activities such as antimicrobial, antitubercular, antiviral, and antimalarial [3-7]. Current research focuses on the development of anticancer drugs with unique structural properties that display distinct cytotoxicity while avoiding

* *Corresponding Author Email: layth.alhayder@gmail.com*

systemic toxic drug effects [8-10]. Thiazole, a 5-membered heterocyclic motif containing sulfur and nitrogen atoms, is of specific interest due to its key role in many medicinally important compounds [11]. Its derivatives have received significant attention for their varied applications as analytical reagents, antioxidants, antifungals, and anticancer agents [12, 13]. They also exhibit diverse pharmacological activities, such as acting as antidepressants [14-18]. The current study examines the synthesis of a novel compound (DEAP) using an array of spectral methods (^{1}H,^{13}C-NMR, Mass, UV-Vis, Infrared FT-IR, XRD, FE-SEM, and C.H.N.S) and assesses its biological activities. In particular, the study evaluates the compound's potential as an anticancer drug, using prostate and breast cancer (MCF-7) cell lines, and contrasts its effects with those on normal cell lines using the MTT assay.

MATERIALS AND METHODS

Chemicals and materials

The subsequent chemicals were obtained commercially and utilized without additional purification: 2-aminothiazol ($C_3H_4N_2S$), 4-aminoacetophenone (C_8H_9NO), benzil ($C_{14}H_{10}O_2$), and 2-aminophenol (C_6H_7NO), sourced from Sigma-Aldrich (Germany). Ethanol Absolute

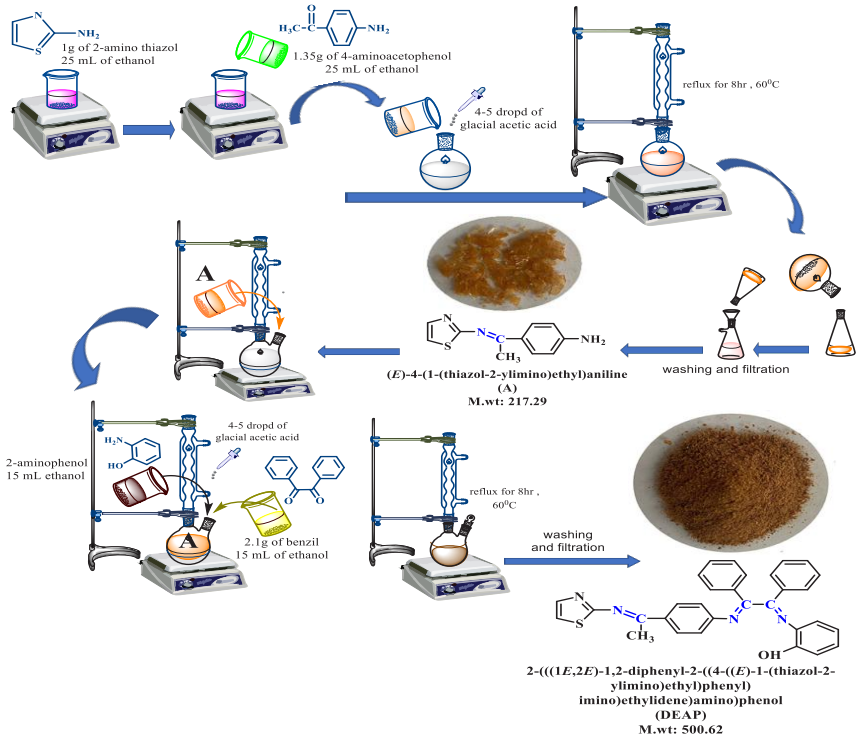

Fig. 1. Preparation of compound (DEAP).

Table 1. Elemental analysis and some physical properties of the Compound (DEAP).

Compound	Color	Molecular Weight (g/mol)	M.P (°C)	Yield %	Molecular Formula	Found (% Cal.)			
						C	H	N	S
DEAP	Brown	500.62	227	87	$C_{31}H_{24}N_4OS$	74.38 74.54	4.83 4.92	11.19 11.43	6.40 6.52

(CH_3CH_2OH) was procured from Scharlau. All reagents employed were of analytical grade purity, requiring no further purification, and all solutions were prepared using deionized water.

Instruments

The chemical (DEAP) was elementally microanalyzed utilizing an EA 300 (C.H.N.S) element analyzer. DMSO-d_6 was the solvent and TMS was the internal reference for 1H and 13C NMR spectra on a Bruker 400 MHZ spectrometer. A Shimadzu Agilent Technologies 5973C at 70 eV produced mass spectra. Using 100% ethanol in a 1 cm quartz cuvette, a T80-PG double beam (UV-Vis) spectrophotometer measured electronic spectra from 200 to 800 nm. A Shimadzu 8400 S captured KBr disk FT-IR spectra (4000400 cm^{-1}). MIRA3 TESCANs captured FESEM images. Bestec Aluminium anode-Germany XRD tests were performed. X-ray diffractometer utilizing (Cu K_α) radiation (1.41.5418 A°) from (5-80°).

Preparation of (DEAP)

The synthesis of compound (DEAP) was accomplished in two stages (Fig. 1). The first stage entailed the creation of compound A, (*E*)-4-(1-(thiazo-2-ylimino) ethyl) aniline. This was prepared by dissolving (1.5 g, 1 mmol.) of 2-aminothiazol in (25 ml) of absolute ethanol, followed by the addition of (1.35 g, 1 mmol.) of 4-aminoacetophenone, also dissolved in (25 ml) of absolute ethanol, while stirring continuously. Post-refluxing the mixture for 8 hours, it was cooled, and a precipitate was observed. The precipitate was filtered, dried, and recrystallized from absolute ethanol, yielding a 73% product with a melting point of 207°C. The second stage involved creating compound DEAP by dissolving compound A (2.1 g, 1 mmol.) in (15 ml) of absolute ethanol. To this, a solution of benzil (2.1 g, 1 mmol.) and 2-aminophenol (1g, 1 mmol.), each dissolved in absolute ethanol (25 ml and 15 ml, respectively), was added while continuously stirring. Additionally, 4-5 drops of glacial acetic acid were introduced into the mixture. After refluxing this mixture for 8 hours and subsequently cooling it, a precipitate formed. This was filtered, dried, and recrystallized from absolute ethanol, leading to the formation of compound (DEAP) 2-(((1*E*,2*E*)-1,2-diphenyl-2-((4(*E*-1-(thiazol-2-ylimino) ethyl) phenyl) imino) ethylidene) amino) phenol as a solid

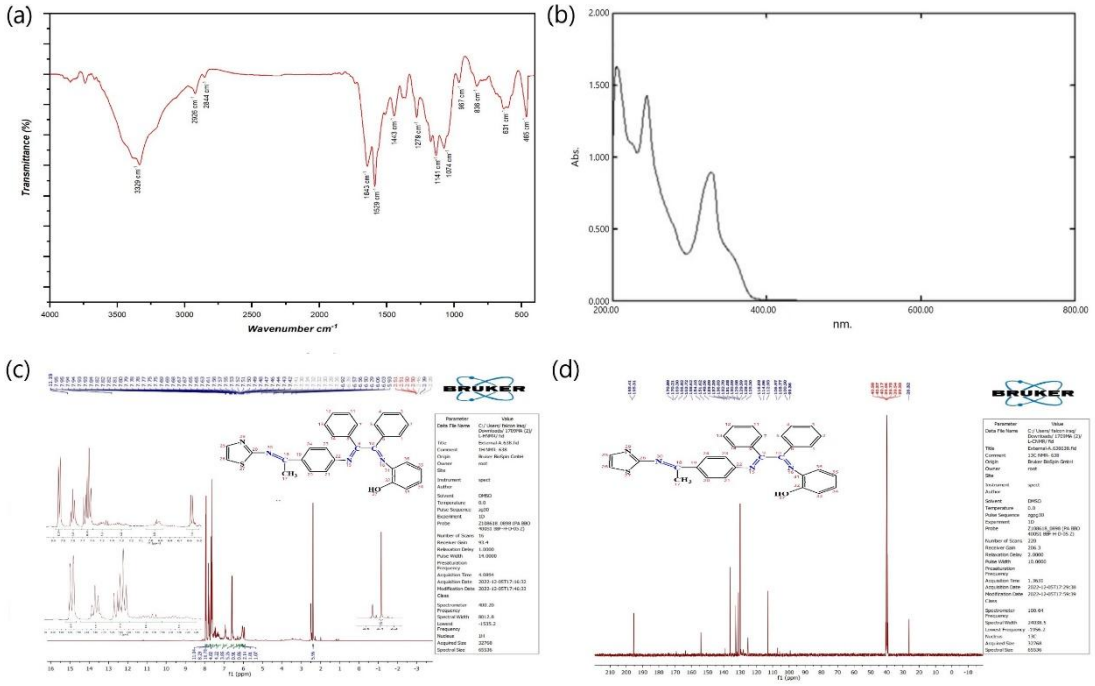

Fig. 2: FT-IR spectra (a), UV–Vis spectrum (b), and ^{1}H,^{13}C-NMR (c,d) of compound (DEAP)

brown product with an 87% yield and a melting point of 227°C. Elemental analysis was consistent with the formula for compound (DEAP) presented in Table 1.

RESULTS AND DISCUSSION

The functional groups have been confirmed via Fourier-transform infrared spectroscopy (FTIR) analysis[19], Fig. 2a: showed the band at 3329cm^{-1} for (OH) phenol, 2926 cm^{-1} for (C-H) Aromatic, 2844 cm^{-1} for (C-H) Aliphatic , 1529 cm^{-1} for (C=N) thiazole ring, 1643 cm^{-1}for (C=N) imine , 1443 cm^{-1} for (C=C) Aromatic, 1279 cm^{-1} for (C-S). UV–visible absorption spectrum was obtained at room temperature for the compound (DEAP), in Fig. 2b includes three absorption peaks, two of which are two peaks at 205 nm (148780 cm^{-1}) and 244 nm (40984cm^{-1}) which are due to the π-π* type transition resulting from the presence of rings vinyl. While the third peak at 327 nm (30581cm^{-1}) indicates the n-π* type transition, and this is due to each of the azomethine groups of the Schiff base and the thiazole ring[20]. The nuclear magnetic resonance (NMR) spectroscopy was used to identify the placement of protons in the obtained compound (DEAP), ^{1}H-NMR (DMSO-d_6) Fig. 2c: showed δ:11.19 (S,1H,OH) phenol, 7.51-7.82 (M,2H,CH) thiazole ring, 6.90, 6.65, 6,92 ,7,26 (M,4H,CH) phenyl ring,7.61,7.69,7.93-7.95 (M,10H,CH) benzil, 7.3,7.79 (M,4H,CH) benzylidenimine, 2.46 (S, 3H, CH_3) methyl group .^{13}C-NMR (DMSO-d_6) Fig. 2d: show,169.28ppm(C_{18}), 195.39ppm(C_{28}), 139.07ppm(C_{31}), 130.07ppm($C_7C_{14}C_1C_5$), 131.91ppm($C_{12}C_6C_3$), 129.97ppm($C_{24}C_{20}C_{11}C_{13}C_4C_{15}$), 128.14ppm($C_{33}$), 112.92ppm ($C_{26}$), 106.95ppm ($C_{36}$), 163.7ppm ($C_{22}$), 154.09ppm ($C_9C_{10}$) ,139.07ppm ($C_{32}$) ,26.32ppm ($C_{17}$) [21-27].

The molecular weight of the Schiff base, as examined in DMSO solvent, was verified through mass spectral analysis [28, 29]. The mass spectra illustrated a parent peak at m/z 500.62 for the [M+H] ion of the compound (DEAP) as depicted in Fig. 3, aligning with the anticipated molecular weight, thereby validating the synthesis of DEAP.

X-ray diffraction elucidates the molecular or atomic arrangement in solid-state materials. Compound (DEAP)'s X-ray diffractograms were computed, and the intensity of diffracted CuKα radiation was measured in 2Θ between 5° and 80° (λ = 1.54060 Å; generator settings 30 mA/40 kV) [30, 31]. The Xpert High Score software calculated diffraction spectra parameters using identified diffraction peaks, revealing the compound's crystalline nature (Fig. 4a). Major relaxes and corresponding d-spacing values were calculated using Bragg's equation (nλ = 2dsinΘ), with d-spacing of 7.05A° at 2Θ = 12.55. The Debye-Scherrer

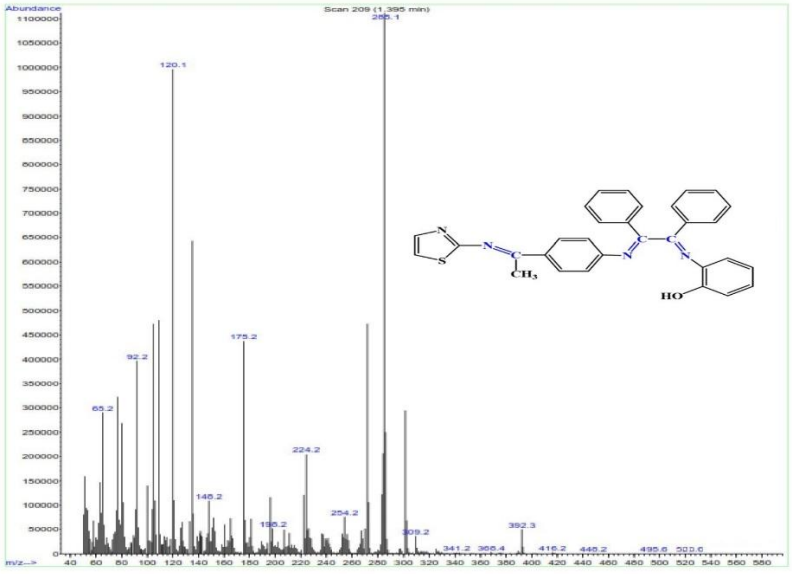

Fig. 3: Mass spectrum of compound (DEAP)

equation (D = kλ/βCosΘ) calculated average crystallite size and size distributions, resulting in an average size of 39.07nm for DEAP. This suggests nanostructure properties due to the crystallite size. Field Emission Scanning Electron Microscopy (FE-SEM) revealed surface morphology, particle shape, aggregation, and distribution in compound (DEAP). The EDX spectrum (Fig. 4b) confirmed the presence of C, O, S, and N elements. The technique operated at a cross-sectional distance of 200nm and magnification force of 20.00 KX. The FE-SEM images (Fig. 4c) showed spherical crystals with an average particle size of 25.98nm, less than 100nm, indicating a nanoscale range. The increased surface area may facilitate the creation of new energy levels, enabling more free electron movement. The compound's characteristics suggest potential use in medical applications, particularly in inhibiting various types of cancers[32-35].

Biological Activities

Thiazole core is integral to several clinically used anticancer drugs including dasatinib, dabrafenib, ixabepilone, patellamide A, and epothilone. Thiazole compounds demonstrate substantial efficacy in inhibiting various types of bacteria and fungi. Their effectiveness can be attributed to their ability to dissolve the outer cell wall, causing fluid loss and eventual cell death. The hybrid atoms, nitrogen and sulfur, bind to specific elements within the cell, such as copper, cobalt, iron, zinc, monovalent manganese, and monovalent potassium ions, which are essential for the bacterial cell. This interaction forms complexes with these elements, leading to cell death due to the depletion of these components [36, 37].

Minimum inhibition concentration)MIC)

Culture media

Prepared according to the manufacturing company instructions were autoclaved at 121°C for 15 minutes at 15 pounds per square inch (Psi).

a- Nutrient broth: used for bacterial activation, a single colony from old culture bacteria add to 3ml of nutrient broth after that, there were incubated for 24h at 37°C.

b- Mueller-Hinton broth: used to activate bacteria and make different compound

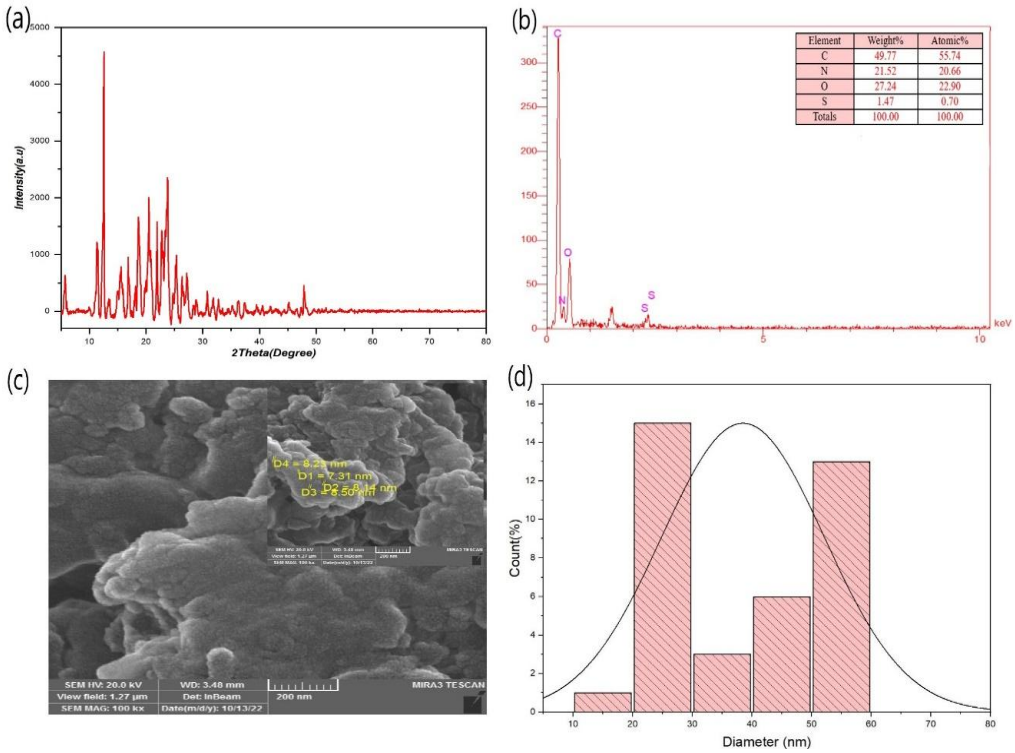

Fig. 4: XRD pattern (a) and EDX analysis (b) and FE-SEM image and grain size histograms (c,d) of compound (DEAP).

concentrations.

Resazurin: (Alamar Blue) solution was prepared by dissolving 0.015 g of resazurin in 100 ml sterile distilled water, a vortex mixer was used until well dissolved and stored at 4°C for a maximum of one week after preparation.

Compound (DEAP) was prepared at double serial dilutions (128-1024 µg/ml) from a 10mg/ml stock solution in a microliter plate, utilizing Mueller-Hinton broth as a diluent. All wells were inoculated with a 20µL bacterial suspension equivalent to McFarland standard no.0.5 (1.5×10^8 cfu/mL), excluding the negative control wells. The microliter plates were incubated at 37°C for a period of 18-20 hrs. Post incubation, 20 µL of resazurin dye was added to all wells, and a further incubation for 2 hours was conducted to observe any color transitions. The sub-MIC concentrations were visually determined in broth micro dilutions as the lowest concentrations exhibiting a color shift from blue to pink in the resazurin broth assay [38, 39].

Determination of compound (DEAP) MIC

The broth microdilution method was used to determine the MIC of the compound (DEAP) in a 96-well microtiter plate. The susceptibility of the five isolates, *Staphylococcus aureus*, *streptococcus mutans*, *pseudomonas aeruginosa*, *E. coli,* and *candida albican* were tested by determining the MIC using a microtiter plate. The results showed that the concentration range from (256-512 µg/ml) to compound was the MIC which can inhibit the growth of *Staphylococcus aureus*, while the MIC of *streptococcus mutans* range between (512-1024 µg/ml) this for gram-positive bacteria. The results showed that the MIC of *E. coli* ranged from (256-512µg/ml) and for pseudomonas aeruginosa multidrug resistance the MIC ranged between (512-256 µg/ml)· finally, The MIC of *candida albican* ranged from (256-512 µg/m) the MIC for a compound to different pathogenic bacteria was shown in Table 2 and Fig. 5.

Antibacterial activity of the compound (DEAP)

The agar well diffusion method was used to detect the antibacterial activity of compound R against four isolates of pathogenic bacteria and one fungal at the MIC concentration according to Lewus [40].

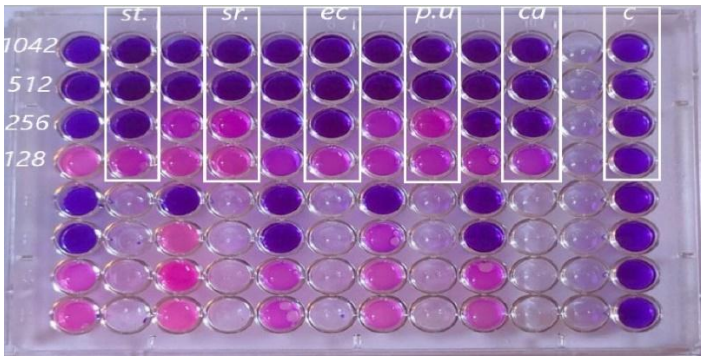

Fig. 5: The MIC of compound (DEAP)

Table 2. The MIC and sub-MIC of Compound (DEAP).

Isolates	(DEAP) MIC (µg/mL)	(DEAP) sub-MIC (µg/mL)
Staphylococcus aureus	256	128
streptococcus mutans	512	256
E. coli	256	128
pseudomonas aeruginosa	512	256
candida albican	256	128

1- Each bacterial isolate under study was grown in nutrient broth and incubated at 37 ºC for 18-24 hrs.

2- After the incubation period, a volume of 0.1 ml of each bacterial suspension was spread on the surface of nutrient agar at 37ºC for 24 hrs.

3- Single colony was added into a test tube having 5 mL of normal saline to yield a bacterial suspension of modest turbidity likened to the standard turbidity solution; this nearly equals $1.5x10^8$ *cfu*/mL

4- Using a sterile cotton swab, a part of the bacterial suspension was transported cautiously and regularly spread on Mueller- Hinton agar medium then left for 10 min.

5- Five millimeter in diameter wells were made in the previous agar layer (3 wells per plate). The agar discs were removed, 50 µL of compound (DEAP) was added to each well using a micropipette, and the D.W was added to the middle well as a control. Plates were incubated at 37 ºC for 18 hrs. and after that, the diameter of inhibition zones was recorded. Table 3 showed the antibacterial activity assay of the compound (DEAP) at the MIC concentration of each isolate. The results indicated that DEAP compound has higher antibacterial activity against all pathogenic isolates. The difference in the biological activity of the compound (DEAP) is attributed to the resistance and sensitivity of bacterial isolates. Second, the difficulty and ease of dispersal of compounds in the culture medium, and finally, the solubility of the compound (DEAP) [41].

Cytotoxic activity

The Freshney method was utilized to cultivate both prostate and breast cancer cell lines. The cells were dissolved using a 37°C water bath, subsequently being positioned in a 25 cm^2 animal cell culture dish, containing RBMI-1640 culture medium and 10% calf serum. The culture dishes were incubated in a 5% carbon dioxide environment at 37°C for 24 hours. Post incubation, secondary cultures were created upon confirming uncontaminated cellular growth. The viability and contamination-free status of all cells were ensured via examination with an inverted microscope, confirming they had proliferated to the required number, approximately 1000 cells/ml. The prepared cells were relocated to a structure referred to as the growth cabin. The used culture medium was disposed of and the cells were cleansed with Physiological Saline Solution (PBS), a procedure repeated twice, each iteration lasting 10 minutes, after that, a sufficient amount of the enzyme trypsin was added to these cells and incubated for 30-60 seconds at a temperature of 37 °C. They were placed under observation until they changed from monolayer to single cells. At that time, the enzyme was stopped by adding a new growth medium containing blood serum cow-calf, after that, these cells were collected in the tubes of the centrifuge and placed in the device at a speed of 2000 rpm for ten minutes at room temperature, to precipitate the cells and get rid of trypsin, and the culture medium used. The filtrate was discarded and the cells were suspended in a new culture medium containing 10% of Calf serum. The filtrate was discarded and the cells were suspended in a new culture medium containing 10% of calf blood serum. After that, many cells were examined by taking a calculated and specific volume of the cell suspension plus the same volume of dye (Trypan Blue) to know

Table 3. Antimicrobial activity data (zone of inhibition in mm) of DEAP.

Isolates	DEAP
E.coli	12 mm
Pseudomonas aeruginosa	12 mm
Streptococcus mutans	15 mm
Staphylococcus aureus	15 mm
Candida albican	14 mm

Highly active = (inhibition zone >12 mm).
Moderately active =(inhibition zone 9– 12 r
Slightly active = (inhibition zone 6– 9 m

the total number of cells and the percentage Vital using a slice (Hemocytometer) and according to the equation below:

$$C = N \times 10^4 \times F/ml \quad (1)$$

Where C is the number of cells present in 1mL of the solution, N is the number of cells on the slide, F is the mitigation factor, and 104 is the slide's dimensions. Then the vital percentage of cells in the sample was calculated using slide (Hemocytometer) according to the equation shown below, and the cell suspension was distributed in new containers and incubated in a 5% incubator of (CO_2) at a temperature of 37°C, for (24) hours.

Vitality percentage of living cells = live cells/ dead cells x 100

Test the Dye of MTT To Examine the Vitality of Cells
Principle of Testing
Test principle

The MTT method is used to detect the biological activity of anti-cancer compounds, through which the extent of the toxicity of chemicals on cells outside the body of the organism is revealed through electronic transmission of the plasma membrane, and to determine the effect of these substances and how to use them as a treatment if their toxicity towards infected cells is shown, provided that they are not effective on average, uninfected cells.

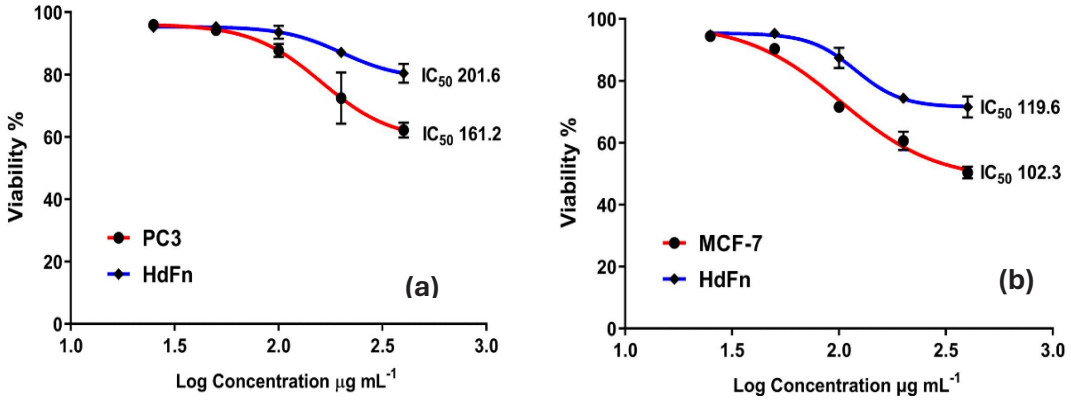

Fig. 6: LC 50 (µg/ml) values of compound (DEAP) (a) PC3 cells and (b) MCF-7 cells lines with the normal cell line

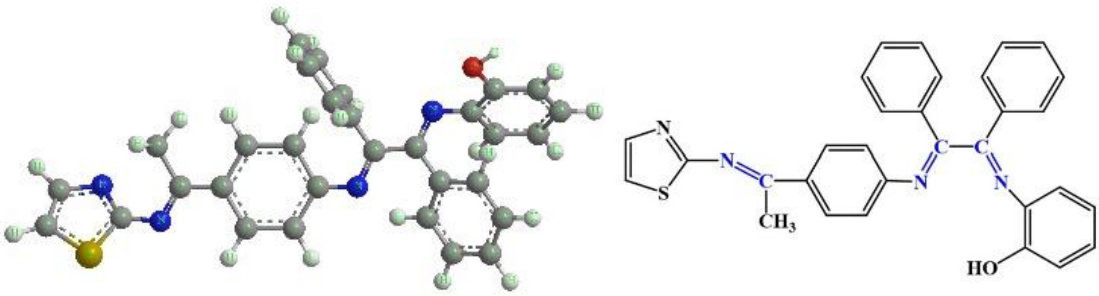

Fig. 7. Proposed structural formula of compound (DEAP).

Tetrazolium salts are considered one of the indicators for measuring the level of activity of cells in prokaryotic organisms as well as eukaryotic organisms, assays are usually performed 3-(4,5 Dimethyl thiazol- 2-yl)-2,5-Diphenyl Tetrazolium Bromide (MTT)in the dark because the MTT detector is light sensitive, Where the percentage of live cells can be calculated through a colorimetric assay to measure the activity of cellular enzymes that reduce Tetrazolium dye in MTT after its conversion to blue-purple formazan is insoluble after the MTT dye changes color from yellow and is converted to blue-purple, as a result, increasing the intensity of the blue color means getting the largest number of live cells.

The color change is due to the production of an enzyme called dehydrogenase by the mitochondria, which is responsible for breaking the tetrazolium ring of the MTT dye. The anti-cancer activity of the compound (DEAP) was conducted by cell cytotoxicity and screening for in vitro antitumor activity against prostate cancer line PC3 and breast cancer (MCF-7) cell lines were evaluated by determining their cellular viability using the colorimetric (MTT) assay.

The Method of Work

Cancer line cells were processed by following the same steps described in paragraphs (2-18-1); then, the cellular suspension was placed in a plate containing 96 holes with a flat base, and it was incubated in an incubator with CO2 5% at a temperature of 37 °C for a full day (24 hours). After that, 100 microliters of that suspension were added in each hole, then the prepared concentrations of the compound under study were added (12.50, 25, 50, 100, 200, and 400 µg/ml) to the pits, at the rate of (3) pits for each concentration, after which the plate was incubated for 24 hours, i.e., a full day, and the incubation temperature was 37°C, and 10 microliters of MTT solution was added to each well, at a concentration of 0.45 mg/ml. Then the plate was incubated again for 4 hours at a temperature of 37°C; after that, 100 ***µL*** of solubilization solution was added to dissolve the Formazan Crystal solution. Finally, the absorbance of that sample was read at wavelength 570 nm using an ELASIS device.

Chemotherapy is the primary method for treating metastasized cancers. The compound (DEAP) have been screened for its anticancer property against breast cancer (MCF-7) cell lines and prostate cancer (PC3) using five different concentrations, and their effect on the normal cells (control) was also checked and operated by (MTT) protocol [42, 43]. Table 4, and Fig. 6 shows the effect of the compound (DEAP) on the growth process of prostate cancer cells (PC3) and normal healthy cells (HdFn). At a concentration of 400 µg/ml for cells of prostate cancer cell lines (PC3) as well as normal cells (HdFn), healthy cells were used to compare with prostate cancer cells (PC3) to find out the possibility of using them as a drug. The reactivity with the organic compound ranged between (96.80% - 71.95%) for PC3 prostate cancer cells, while the percentage ranged between (96.95% - 81.70%) for standard (HdFn) cells. It was found that the best inhibition rate for PC3 prostate cancer cells at The concentration of 400 µg / ml was 28.05%, while the percentage of inhibition of the cell line of healthy cells (HdFn) at the same concentration was 18.3%, which is almost a good result, as we need some modifications to increase this percentage. Among the important things that must be mentioned and that we have reached through the tests that

Table 4. Effect compound (DEAP) on PC3, MCF-7 cells and compared with the normal cell line

Con.(µg.mL^{-1})	compound (DEAP)							
	Cancer line cells of PC3		Normal line cells HdFn		Cancer line cells of MCF-7		Normal line cells HdFn	
	Mean	SD	Mean	SD	Mean	SD	Mean	SD
25	96.80	0.94	96.95	1.14	94.48	0.87	94.83	0.97
50	94.06	1.38	96.49	1.29	90.39	1.36	95.33	1.18
100	93.09	3.74	92.21	2.78	71.61	1.43	87.42	3.25
200	82.91	0.57	87.92	3.58	60.59	2.98	74.38	0.88
400	71.95	3.05	81.70	4.74	50.39	1.88	71.57	3.37

were conducted for the organic compound and among the cells of prostate cancer lines (PC3 and normal cells ((HdFn) is (IC50) the half inhibitory concentration (Inhibition Concentration Fifty), as the half inhibitory concentration reached Fifty (IC_{50}) through the interaction of the organic compound with the prostate cancer cell line (PC3) 161.2 µg/ml, while the half inhibitory concentration of healthy cells (HdFn) was 201.6 µg/mL represents the relationship between the biological activity of the prostate cancer cell line PC3 and cells of the normal cell line HdFn against the concentration of the organic compound. While the breast cancer (MCF-7) cell lines, It was noted that the inhibition percentages for the compound (DEAP) differed according to the type of cell line, as the number of live cells remaining after interaction with the organic compound ranged between (94.48% - 50.39%) for the cells of the breast cancer cell line (MCF-7), and between (94.83% - 71.57%) for cells of the normal cell line (HdFn). The highest percentage of inhibition of the compound (DEAP) appeared in the breast cancer cell line (MCF-7) at a concentration of 400 µg/ml, as the percentage of inhibition after reaction with the organic compound ranged 49.61%, while the highest percentage of inhibition appeared for the compound (DEAP) after The reactance of the normal cell line (HdFn) at the same concentration was 28.43% [29-31].

CONCLUSION

This study documents the synthesis and spectral characterization of a novel Schiff base compound, 2-(((1*E*,2*E*)-1,2-diphenyl-2-((4(€-1-(thiazol 2ylimino) ethyl) phenyl) imino) ethylidene) amino) phenol (DEAP), originating from thiazole, the structure of which is depicted in Fig. 7. The formation of DEAP was validated through FTIR, ^{1}H ^{13}C-NMR, and electronic spectral analysis. Various morphologies of the Schiff base compound were observed via XRD and FE-SEM. Additionally, DEAP exhibited significant biological activity against bacteria, along with selective cytotoxicity, damaging cancerous cell lines without harming normal cells, a property pivotal to future cytotoxic therapies. Findings suggested that such compounds might significantly inhibit the growth of cancer cells, positioning them as promising candidates for further structural modifications and pharmacological assessments. The potential for their application as anti-cancer drugs in medical and pharmaceutical fields is undeniable.

CONFLICT OF INTEREST

The authors declare that there is no conflict of interests regarding the publication of this manuscript.

REFERENCES

1. da Silva CM, da Silva DL, Modolo LV, Alves RB, de Resende MA, Martins CVB, et al. Schiff bases: A short review of their antimicrobial activities. Journal of Advanced Research. 2011;2(1):1-8.
2. Gupta VK, Singh AK, Kumawat LK. Thiazole Schiff base turn-on fluorescent chemosensor for Al3+ ion. Sensors Actuators B: Chem. 2014;195:98-108.
3. Muhammad S, Kumar S, Koh J, Saravanabhavan M, Ayub K, Chaudhary M. Synthesis, characterisation, optical and nonlinear optical properties of thiazole and benzothiazole derivatives: a dual approach. Mol Simul. 2018;44(15):1191-1199.
4. Synthesis and Characterization of New Schiff Base Ligand Derived from 4- aminoantipyrine and its complexes with some metal ions and Their Fluorescence Study. International Journal of Pharmaceutical Research. 2020;13(01).
5. Al-Suraify SMT, Hussien LB. Retraction Note: Synthesis and characterization of new compounds derived from 1H-indol-5-ylamine. Applied Nanoscience. 2024;14(4):719-719.
6. Synthesis of New Nitrogenous Derivatives Based On 3-Chloro–1-methyl-1H-indazole. International Journal of Pharmaceutical Research. 2020;12(sp1).
7. Al-Suraify SMT, Hussien LB. RETRACTED ARTICLE: Synthesis and characterization of new compounds derived from 1H-indol-5-ylamine. Applied Nanoscience. 2022;13(3):2083-2092.
8. Malekshah RE, Shakeri F, Khaleghian A, Salehi M. Developing a biopolymeric chitosan supported Schiff-base and Cu(II), Ni(II) and Zn(II) complexes and biological evaluation as pro-drug. Int J Biol Macromol. 2020;152:846-861.
9. Synthesis of Poly(methacrylic acid)/Montmorillonite Hydrogel Nanocomposite for Efficient Adsorption of Amoxicillin and Diclofenac from Aqueous Environment: Kinetic, Isotherm, Reusability and Thermodynamic Investigations. American Chemical Society (ACS).
10. Synthesis and Characterization of Novel Compounds Derived From 6-methyl-2,6 dihydro[1,2,4-triazino[4,3-b] indazol-3(4H)-one. International Journal of Pharmaceutical Research. 2020;12(sp1).
11. de Santana TI, Barbosa MdO, Gomes PATdM, da Cruz ACN, da Silva TG, Leite ACL. Synthesis, anticancer activity and mechanism of action of new thiazole derivatives. Eur J Med Chem. 2018;144:874-886.
12. Abd-Elzaher MM, Labib AA, Mousa HA, Moustafa SA, Ali MM, El-Rashedy AA. Synthesis, anticancer activity and molecular docking study of Schiff base complexes containing thiazole moiety. Beni-Suef University Journal of Basic and Applied Sciences. 2016;5(1):85-96.
13. Jagadeesan S, Karpagam S. Novel series of N-acyl substituted indole based piperazine, thiazole and tetrazoles as potential antibacterial, antifungal, antioxidant and cytotoxic agents, and their docking investigation as potential Mcl-1 inhibitors. J Mol Struct. 2023;1271:134013.
14. Hameed A, al-Rashida M, Uroos M, Abid Ali S, Khan KM.

Schiff bases in medicinal chemistry: a patent review (2010-2015). Expert Opin Ther Pat. 2016;27(1):63-79.
15. More MS, Joshi PG, Mishra YK, Khanna PK. Metal complexes driven from Schiff bases and semicarbazones for biomedical and allied applications: a review. Materials Today Chemistry. 2019;14:100195.
16. Ali MM, Mhaibes RM, Othman MA-M, R. Lahhob Q, Qasim MJ. Association between triglyceride-glucose index and risk of chronic kidney disease: a systematic review and meta-analysis. Journal of Nephropharmacology. 2024;13(2):e12692.
17. Hashim Al-Zuhairy S, Abed Darweesh M, Abdul-Mounther Othman M, Al-Huda Salah Al-Zuhairy N. Vitamin D deficiency in young children with iron deficiency in Misan province, Iraq. J Med Life. 2022;15(3):387-391.
18. Hmood NA, Mother Othman DMA, Mohsin Ali DM. Transcription Factor 7-Like 2 Gene Polymorphisms rs7903146associationwith Type 2 Diabetic Polycystic Ovarian Syndrome Women of Iraqi Population. Annals of Tropical Medicine and Public Health. 2019;22(12):156-164.
19. jasim A, Adnan S. Preparation, characterization and study the biological activity for (six and seven) membered heterocyclic derivatives from 6-methoxy-2-amino benzo thiazole. AIP Conference Proceedings: AIP Publishing; 2023. p. 030009.
20. Saydam S. Synthesis And Characterisation of the New Thiazole Schiff Base 2-(2-Hydroxy)Naphthylideneamino-Benzothiazole and Its Complexes With Co(Ii), Cu(Ii), And Ni(Ii) Ions. Synth React Inorg Met-Org Chem. 2002;32(3):437-447.
21. Issa YM, Hassib HB, Abdelaal HE. 1H NMR, 13C NMR and mass spectral studies of some Schiff bases derived from 3-amino-1,2,4-triazole. Spectrochimica Acta Part A: Molecular and Biomolecular Spectroscopy. 2009;74(4):902-910.
22. Khan MI, Khan A, Hussain I, Khan MA, Gul S, Iqbal M, et al. Spectral, XRD, SEM and biological properties of new mononuclear Schiff base transition metal complexes. Inorg Chem Commun. 2013;35:104-109.
23. Batool M, Haider MN, Javed T. Applications of Spectroscopic Techniques for Characterization of Polymer Nanocomposite: A Review. Journal of Inorganic and Organometallic Polymers and Materials. 2022;32(12):4478-4503.
24. Jamel HO, Jasim MH, Mahdi MA, Ganduh SH, Batool M, Jasim LS, et al. Adsorption of Rhodamine B dye from solution using 3-((1-(4-((1H-benzo[d]imidazol-2-yl)amino) phenyl)ethylidene)amino)phenol (BIAPEHB)/ P(AA-co-AM) composite. Desalination and Water Treatment. 2025;321:101019.
25. Al-Adilee KJ, Atyha SA. Synthesis, Spectral, Thermal and Biological Studies of Some Metal Complexes Derived from Heterocyclic Mono Azo Dye Ligand 2'[(2'-Hydroxy-4-methyl phenyl)azo]imidazole. Asian J Chem. 2018;30(2):280-292.
26. Jabbar FA, Jasim LS, Sahib IJ. Characterization, modelling, and kinetics studies of the adsorption of phenol from aqueous solutions onto [ZnO/P(AA-CA)] composite as an adsorbate surface. AIP Conference Proceedings: AIP Publishing; 2023. p. 040002.
27. Majeed HJ, Idrees TJ, Mahdi MA, Abed MJ, Batool M, Yousefi SR, et al. Synthesis and application of novel sodium carboxy methyl cellulose-g-poly acrylic acid carbon dots hydrogel nanocomposite (NaCMC-g-PAAc/ CDs) for adsorptive removal of malachite green dye. Desalination and Water Treatment. 2024;320:100822.
28. Nagesh GY, Mruthyunjayaswamy BHM. Synthesis, characterization and biological relevance of some metal (II) complexes with oxygen, nitrogen and oxygen (ONO) donor Schiff base ligand derived from thiazole and 2-hydroxy-1-naphthaldehyde. J Mol Struct. 2015;1085:198-206.
29. Diao X, Ellin NR, Prentice BM. Selective Schiff base formation via gas-phase ion/ion reactions to enable differentiation of isobaric lipids in imaging mass spectrometry. Analytical and Bioanalytical Chemistry. 2023;415(18):4319-4331.
30. Al-Adilee K, Kyhoiesh HAK. Preparation and identification of some metal complexes with new heterocyclic azo dye ligand 2-[2 – - (1- Hydroxy -4- Chloro phenyl) azo]- imidazole and their spectral and thermal studies. J Mol Struct. 2017;1137:160-178.
31. Kyhoiesh HAK, Al-Hussainawy MK, Waheeb AS, Al-Adilee KJ. Synthesis, spectral characterization, lethal dose (LD50) and acute toxicity studies of 1,4-Bis(imidazolylazo)benzene (BIAB). Heliyon. 2021;7(9):e07969.
32. Waheeb AS, Al-Adilee KJ. Synthesis, characterization and antimicrobial activity studies of new heterocyclic azo dye derived from 2-amino- 4,5- dimethyl thiazole with some metal ions. Materials Today: Proceedings. 2021;42:2150-2163.
33. Kianipour S, Razavi FS, Hajizadeh-Oghaz M, Abdulsahib WK, Mahdi MA, Jasim LS, et al. The synthesis of the P/N-type NdCoO3/g-C3N4 nano-heterojunction as a high-performance photocatalyst for the enhanced photocatalytic degradation of pollutants under visible-light irradiation. Arabian Journal of Chemistry. 2022;15(6):103840.
34. Mahdi MA, Oroumi G, Samimi F, Dawi EA, Abed MJ, Alzaidy AH, et al. Tailoring the innovative Lu2CrMnO6 double perovskite nanostructure as an efficient electrode materials for electrochemical hydrogen storage application. Journal of Energy Storage. 2024;88:111660.
35. Mahde BW, Sultan AM, Mahdi MA, Jasim LS. Kinetic Adsorption and Release Study of Sulfadiazine Hydrochloride Drug from Aqueous Solutions on GO/P(AA-AM-MCC) Composite. International Journal of Drug Delivery TECHNOLOGY. 2022;12(04):1583-1589.
36. Sharma PC, Bansal KK, Sharma A, Sharma D, Deep A. Thiazole-containing compounds as therapeutic targets for cancer therapy. Eur J Med Chem. 2020;188:112016.
37. Sabry MA, Ghaly MA, Maarouf AR, El-Subbagh HI. New thiazole-based derivatives as EGFR/HER2 and DHFR inhibitors: Synthesis, molecular modeling simulations and anticancer activity. Eur J Med Chem. 2022;241:114661.
38. Bharti SK, Nath G, Tilak R, Singh SK. Synthesis, anti-bacterial and anti-fungal activities of some novel Schiff bases containing 2,4-disubstituted thiazole ring. Eur J Med Chem. 2010;45(2):651-660.
39. Blaxland J, Thomas R, Baillie L. The Antibacterial Effect of Humulus lupulus (Hops) against Mycobacterium bovis BCG: A Promising Alternative in the Fight against Bovine Tuberculosis? Beverages. 2022;8(3):43.
40. Lewus CB, Kaiser A, Montville TJ. Inhibition of food-borne bacterial pathogens by bacteriocins from lactic acid bacteria isolated from meat. Applied and Environmental Microbiology. 1991;57(6):1683-1688.
41. Khalil AM, Berghot MA, Gouda MA. Synthesis and antibacterial activity of some new thiazole and thiophene derivatives. Eur J Med Chem. 2009;44(11):4434-4440.
42. Waheeb AS. Spectroscopic, characterization and bioactivity studies of new Ni (II), Cu (II) and Ag (I) complexes with didentate (N,N) donar azo dye ligand. J Mol Struct. 2023;1276:134729.
43. Waheeb AS, Al-Adilee KJ, Al-Janabi AS, Shanmuganathan R, Kadhim MM. Synthesis, characterization, cytotoxic, and computational studies of new complexes (copper and cadmium). J Mol Struct. 2022;1267:133572.